Wind and Structures, Vol. 7, No. 4 (2004) 265-280
DOI: http://dx.doi.org/10.12989/was.2004.7.4.265

Dynamics and instability of the Karman wake mode induced by periodic forcing

Njuki W. Mureithi†

BWC / AECL / NSERC Chair of Fluid-Structure Interaction, Department of Mechanical Engineering, Ecole Polytechnique de Montreal, P.O. Box 6079, Station A Montreal, QC, H3C 3A7, Canada

(Received June 27, 2003, Revised March 7, 2004, Accepted April 6, 2004)

Abstract. This paper presents some fundamental results on the dynamics of the periodic Karman wake behind a circular cylinder. The wake is treated like a dynamical system. External forcing is then introduced and its effect investigated. The main result obtained is the following. Perturbation of the wake, by controlled cylinder oscillations in the flow direction at a frequency equal to the Karman vortex shedding frequency, leads to instability of the Karman vortex structure. The resulting wake structure oscillates at half the original Karman vortex shedding frequency. For higher frequency excitation the primary pattern involves symmetry breaking of the initially shed symmetric vortex pairs. The Karman shedding phenomenon can be modeled by a nonlinear oscillator. The symmetrical flow perturbations resulting from the periodic cylinder excitation can also be similarly represented by a nonlinear oscillator. The oscillators represent two flow modes. By considering these two nonlinear oscillators, one having inline shedding symmetry and the other having the Karman wake spatio-temporal symmetry, the possible symmetries of subsequent flow perturbations resulting from the modal interaction are determined. A theoretical analysis based on symmetry (group) theory is presented. The analysis confirms the occurrence of a period-doubling instability, which is responsible for the frequency halving phenomenon observed in the experiments. Finally it is remarked that the present findings have important implications for vortex shedding control. Perturbations in the inflow direction introduce 'control' of the Karman wake by inducing a bifurcation which forces the transfer of energy to a lower frequency which is far from the original Karman frequency.

Keywords: vortex shedding; period-doubling; wake control; spatio-temporal symmetry; amplitude equations.

1. Introduction

Wind-induced vortex shedding remains an important problem for many engineering structures. Structures susceptible to vortex-induced vibrations include industrial towers, tall buildings, free standing pylons, cables in cable-stayed bridges, power transmission lines, slender marine structures, offshore piles, undersea pipelines etc. A recent review of the role of aerodynamic analysis, over the past five decades, for structural design has been presented by Shiraishi (2002). A review of experimental work on cable aerodynamics of cable stayed bridges may be found in Matsumoto (2002). In the paper, the difficulty associated with the extremely complex 3-dimensional flow field, often compounded by rain, is discussed. An axial flow component for an inclined cable is reported. It is also shown that the axial flow has an important effect on the inclined cable aerodynamics. A

† Associate Professor

quasi-steady theory of the vibration mechanism is also discussed. It is clear that to develop effective damping technology, a fundamental understanding of vortex-structure interaction is needed. Much remains unknown regarding the fundamental wake flow dynamics in the presence of a moving bluff body, particularly the coupled vortex-structure interaction problem.

A fundamental study of 3-dimensional effects in bluff body wakes has provided useful insights into understanding vortex-structure interactions. Transition to 3D flow in a cylinder wake has been experimentally investigated in the excellent body of experimental work by Williamson (1987, 1988, 1989, 1996). The transition is shown to be associated with two axial instability modes (labeled modes A and B). Mode A is found to have a span wise wavelength of 3-4 diameters. Mode B, on the other hand has a smaller wavelength of the order of one diameter. A theoretical study by Barkley and Henderson (1996) has shown that the transition to 3D is the result of instabilities in the flow associated with Modes A and B. The instability modes A and B appear to be closely linked to the axial vortices reported by Matsumoto (2002) for inclined cables.

The 'simpler' essentially 2D problem of vortex-structure interaction remains, at best only partly understood. To model the coupled vortex-structure interaction, classical models were proposed by Hartlen and Currie (1970), and Landl (1975), among others. All wake-oscillators models are based on the observation that the Karman make closely approximates a sinusoidal oscillator for a fixed structure. A van der Pol type nonlinear oscillator can thus be easily adapted to give the dynamical behaviour in this case. Sarpkaya (1979) in a seminal review showed that despite the success of wake oscillator models to predict the structural response amplitude, a closer investigation showed that prediction of lift and drag forces as well as force-structure phase difference was generally poor. Furthermore some of the hysteresis effects observed in experiments could not be predicted by the oscillator models. Mureithi, *et al.* (2000, 2001) recently performed a model perturbation analysis in parameter space. Based on a continuation analysis, it was shown that some of the hysteresis effects could be obtained.

It is clear from the foregoing that the full 3D problem and even the simpler 2D coupled vortex-structure interaction problem remains poorly understood. To this end, the simpler intermediate 2D problem of controlled (forced) cylinder motion in flow has been considered. By having the cylinder execute controlled motion, the coupled fluid-structure problem is partially simplified. It becomes possible to investigate in some detail the direct effect of structural motion on the flow, without the added complication introduced by the feedback mechanism where the flow in turn affects the structural motion.

A number of important reviews on controlled wake dynamics exist. These include Bearman (1984), Griffin and Hall (1991) and Rockwell (1998). Classical works on forced cylinder excitation include Den Hartog (1934), Bishop and Hassan (1964), Koopman (1967), Griffin (1971) and Stansby (1976). Recent work based on transverse cylinder excitation includes, among others, Ongoren and Rockwell (1988), Williamson and Roshko (1988), Blackburn and Henderson (1999), Hover, *et al.* (1998). Rather than mechanical excitation, direct flow excitation (suction and blowing) was employed by Williams, *et al.* (1992) and Park, *et al.* (1994). Rotational oscillations were employed by Baek, *et al.* (1998, 2000, 2001), as well as Tokumaru and Dimotakis (1991).

The earliest work reported was primarily concerned with the dynamics of the cylinder wake under harmonic forcing. The test cylinder was oscillated transverse to the flow at or near the vortex shedding frequency; this corresponds to the lock-in frequency band. Bishop and Hassan (1964) for instance reported a significant increase in the vortex-induced fluid force suggesting enhanced vortex-structure coupling for forced motion. In later works, the excitation frequency range was

expanded beyond the primary lock-in region to include forcing at subharmonics and superharmonics of the shedding frequency. Stansby (1976) for instance reported the occurrence of lock-in or synchronization for $f_K/f_{K0} = 2/1$ and $f_K/f_{K0} = 3/1$ besides the commonly known fundamental harmonic lock-in at $f_K/f_{K0} = 1/1$; here f_{K0} is the stationary cylinder shedding frequency while f_K is the cross-flow forcing frequency. Interestingly, 'stronger' resonance was found to occur for higher order $f_K/f_{K0} = 3/1$ forcing compared to the $f_K/f_{K0} = 2/1$ forcing. This lack of $2/1$ and its cousin $1/2$ synchronization would be later reported in work by Williamson and Roshko (1988). The latter put forward symmetry arguments showing that $f_K/f_{K0} = 2/1$ or $1/2$ synchronization could not occur in a 'steady state'. A more mathematical approach to the same problem was put forward by the author (Mureithi, *et al.* 2003). A symmetry group analysis of the interacting flow 'modes' indicated incompatibility (hence lack of synchronization) when the forcing mode was at half or double the Karman shedding mode.

The observation of multiple lock-in regimes, both superharmonic and subharmonic is the hallmark of wake dynamics during forced cylinder excitation. Complex symmetrical patterns are observed in the excited wake; observation of clearly defined patterns, with a finite number of vortices shed per cycle of cylinder oscillation have led to mode names such as the 2S and 2P modes (S- single vortex, P- pair of vortices), the P+S modes, the 2S+2P mode etc; these identifications were proposed by Williamson and Roshko (1988) and adopted by Krishnamoorthy, *et al*. (2001) among others. These complex patterns exist not just for transverse cylinder excitation but also for excitation in the flow direction. In Williams, *et al.*'s experiments, excitation of the boundary layer was achieved by the unsteady bleed technique introducing perturbations at $\pm 45^o$ from the forward stagnation line. Reflection-symmetric (inflow) forcing was found to significantly affect the mean velocity profile in the wake. Modes corresponding to frequency sum and differences were observed. There is significantly less work reported for inflow excitation compared to cross-flow excitation. The work of Williams et al. and Ongoren and Rockwell suggests that in some sense, possibly due to the inherent instability of the symmetrical wake (induced by inline excitation), symmetrical forcing in the flow direction may lead to an even more complex problem. Indeed this is the case for flexible structure case. While a single lock-in frequency is commonly identified for cross-flow problem, the dynamics are much more complex for coupling between the symmetrical shedding and the inflow vibration of the structure. This complexity is clearly captured in the following description (of the dynamics) by King (1977), ".... the ratio of cylinder (to flow periodicity) frequency apparently slips into convenient numbers, 7:2, 3:1, 7:3, 13:6 ...". This suggests significantly more complex fluid-structure interaction in the inflow direction compared to the cross-flow direction where the 1:1 lock-in is dominant.

The problem of *inflow* wake excitation is the primary subject of this work. The secondary subject is the general problem of wake response to forced excitation.

We report on both experimental tests and a theoretical analysis of forced wake excitation. In the experiments both hot-wire measurements and flow visualization of a cylinder wake are presented. The cylinder is mechanically forced in flow at rational frequency ratios of the shedding frequency. Inflow cylinder oscillations are considered. Theoretically, the structure of the expected modal amplitude equations is presented based on a group theoretic analysis. Next, a stability analysis of one modal amplitude equation is performed with the second mode as a control parameter. The relation between the theoretically predicted stability behavior and actual test results provides a litmus test for the analysis. The main results here were presented at AWAS 2002, (Mureithi 2002).

2. Experimental tests

2.1. Test setup

Tests were conducted in a miniature wind tunnel test section 0.55 m long and 0.1×0.1 m in cross-section, Fig. 1. Tests were usually conducted at a fixed flow velocity and $\mathrm{Re} \approx 2000$. The test cylinder having diameter $D = 20$ mm could be mechanically oscillated at the desired amplitude and frequency. The cylinder aspect ratio was 1:5; the cylinder spanned the complete test section eliminating 3D end effects. The blockage ratio in the wind tunnel is approximately 20%. A few tests (at higher Reynolds number) were also done with a $D = 10$ mm cylinder; corresponding to a 50% decrease in blockage to 10%. These tests gave results similar to those obtained with the larger cylinder; hence, the period-doubling instability (see below) was also obtained. Hence, although blockage effects certainly alter the local characteristics of the flow, the global dynamics are not significantly changed. The steady drag is also higher due to blockage; however, this is a steady quantity, which does not affect the dynamic wake stability. As shown in the results below, dynamical quantities such as the Strouhal number ($S \approx 0.2$) are close to values found for the case of no blockage. This should clearly be the case since the symmetry of the system is unchanged. Thus, basic (symmetry dependent) results, which are of primary interest here, should not change significantly.

The cylinder is visible within the test section in Fig. 1. Cylinder excitation was in the direction parallel to the flow achieved by means of a shaker seen in the figure. A hot-wire probe, located 2.25D downstream of the test cylinder and offset 0.5D from the centerline, was used to measure local wake flow velocity fluctuations. Flow visualization tests were also done. An oil coated nickel-chromium wire at the test section entrance, on heating, introduced smoke streaks into the test section. Regular vegetable oil was used for smoke generation.

2.2. Test results

Fig. 2 shows the typical wake structure behind the stationary cylinder. The natural vortex

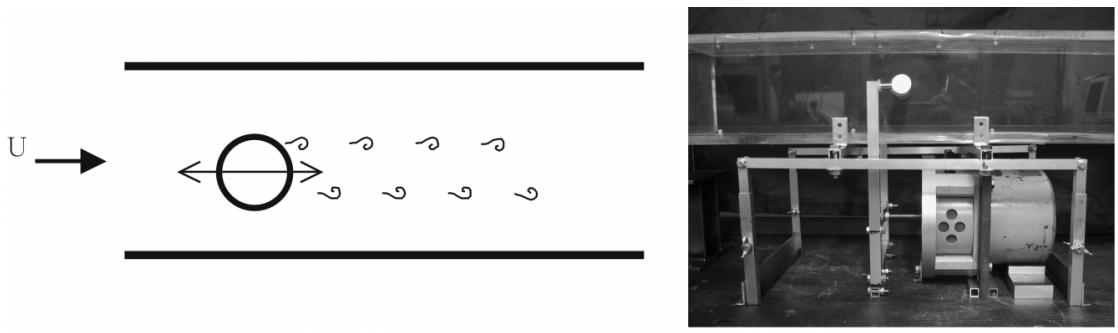

(a) Schematic showing single cylinder in wind-tunnel subjected to transverse flow

(b) The actual test cylinder the wind-tunnel test section; the shaker is also visible

Fig. 1 (a) Schematic showing single cylinder in wind-tunnel subjected to transverse flow and (b) the actual test cylinder in the wind-tunnel test section; the shaker is also visible.

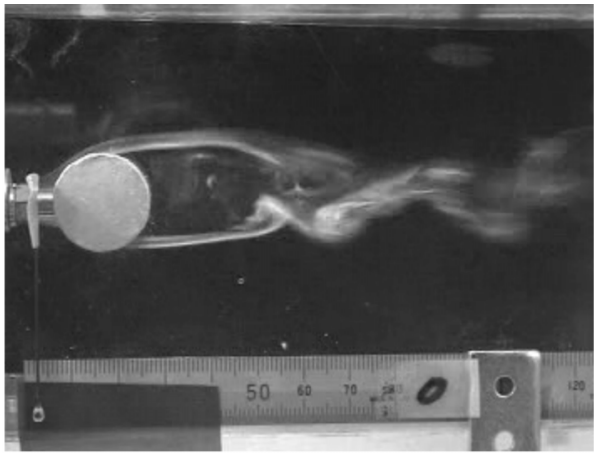

Fig. 2 Wake structure behind a stationary cylinder (Re=1918).

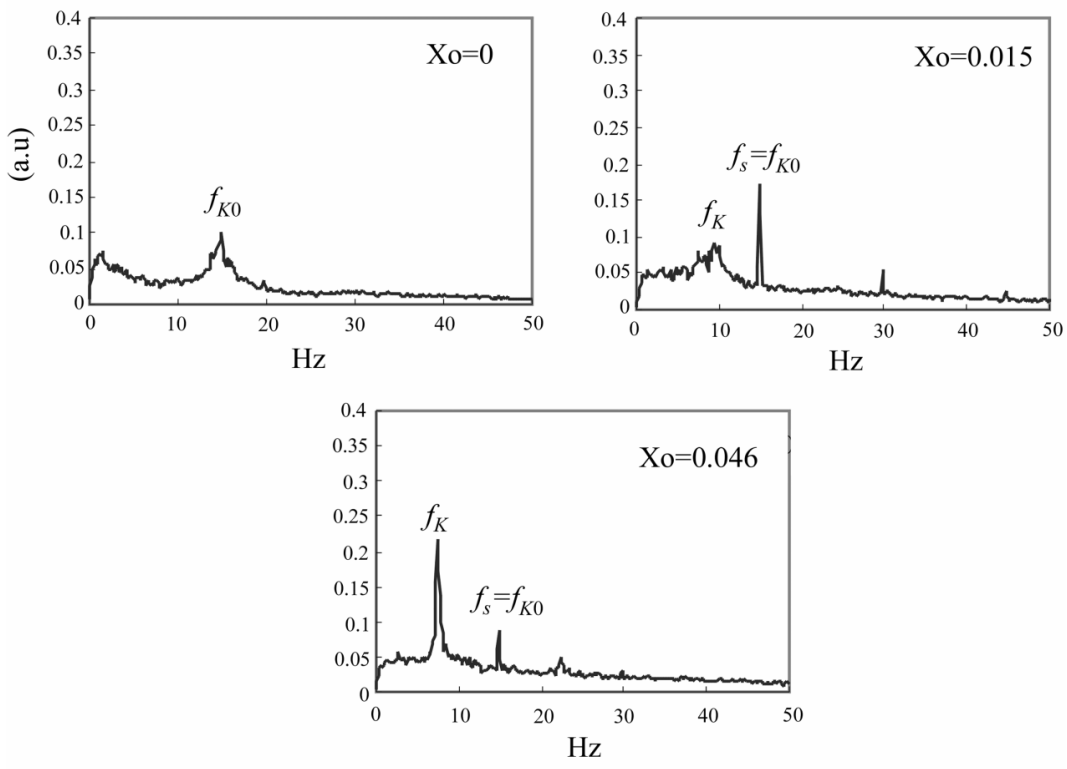

Fig. 3 Wake velocity spectra for $f_S=f_{K0}$ forcing. Dimensionless forcing amplitudes are shown. The important frequencies shown are, f_{ko}: shedding frequency for stationary cylinder; f_s: cylinder oscillation frequency, f_k: dominant wake frequency during cylinder oscillations.

shedding frequency for a stationary cylinder is $f_{K0}=15$ Hz. The Reynolds number is 1918. In Fig. 3 sample power spectra for $U=1.45$ m/s are presented. The cylinder is mechanically forced to oscillate at

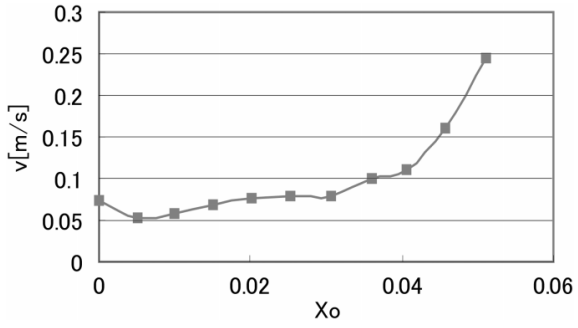

Fig. 4 Variation of local fluctuating wake velocity v with X_0 for $f_S/f_{K0}=1$

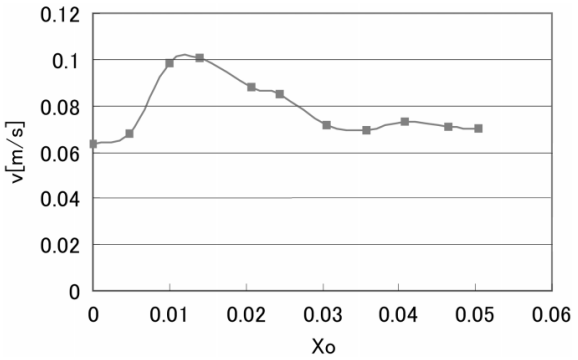

Fig. 5 Variation of local fluctuating wake velocity v with X_0 for $f_S/f_{K0}=2$

$f_S = f_{K0} = 15$ Hz in the inflow direction. In all test results, the cylinder displacement is given by X_0, which is the cylinder oscillation amplitude non-dimensionalized by the cylinder diameter. For $X_0=0.030$, a second smaller peak appears near f_S. This new frequency is the modified shedding frequency f_K. As X_0 increases, f_K drifts away from the forcing frequency f_S. At high enough values of X_0, the shedding frequency locks into half the forcing frequency. This suggests the occurrence of a subharmonic instability, a nonlinear phenomenon where the original wake now oscillates at half the cylinder forcing frequency, $f_K = f_S/2 = f_{K0}/2$. This instability is also referred to as a period-doubling instability in the field of nonlinear dynamics. It is one of the fundamental instabilities or bifurcations found to occur in nonlinear systems. The subharmonic response at $f_K = f_S/2$ is found to persist for higher forcing amplitudes $X_0 > 0.036$. For $X_0 \geq 0.046$ the subharmonic response is dominant.

The results for two tests with $f_S = f_{K0} = 15$ Hz and $f_S = 2f_{K0} = 30$ Hz, respectively, are summarized in Figs. 4 and 5. In these figures the variation of the rms flow velocity perturbation component v at f_K is plotted versus the cylinder amplitude X_0. These figures represent the wake dynamic response at the dominant frequency f_K. Note that the dominant frequency f_K is, however, amplitude dependent, approaching $f_S/2$ for higher amplitudes.

Further tests were conducted in the frequency range $1 < f_S/f_{K0} < 3$. The subharmonic instability was found to persist in all cases. Wake/forcing frequency ratios f_K/f_S plotted versus f_S/f_{K0} in Fig. 6 confirm this finding. In this figure, the results of a second test are also plotted. Period-doubling is clearly evident in the range $1 \leq f_S/f_{K0} \leq 1.75$. The wake consistently oscillates at only half the forcing frequency. For $f_S/f_{K0} > 1.75$, the subharmonic frequency drops further. Thus $f_K/f_S \approx 1/3$ near $f_S/f_{K0} = 2.25$ while $f_K/f_S \approx 1/4$ for $f_S/f_{K0} = 2.75$. The ratio $f_S/f_{K0} = 2$ appears to be a transition state. Hence, while for one of the tests clear period-doubling occurs, the frequency ratio drops to closer to 1/3 in the second test.

The frequency results above were supported by flow visualization results. The wake structure for $f_S/f_{K0} = 1$ forcing in Fig. 7, Re=1918, can be contrasted to the stationary cylinder wake structure in Fig. 2. It takes one cylinder cycle for the lower vortex to be shed. Consequently, wake velocity perturbations occur at half the cylinder frequency.

Fig. 8 shows the wake structure for forcing at double the shedding frequency $f_S/f_{K0} = 2$; shots are taken one cylinder cycle apart (twice the vortex shedding frequency). The near wake is clearly

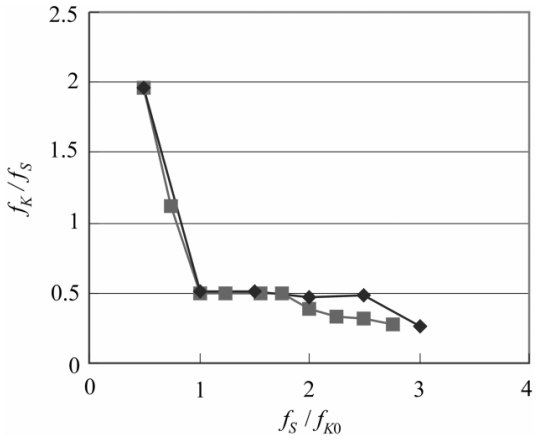

Fig. 6 Wake/forcing frequency ratio versus forcing/natural shedding ratio

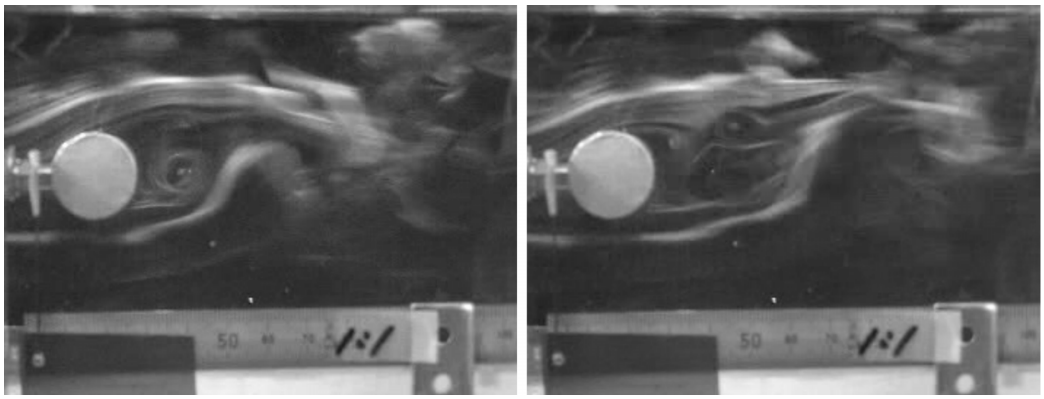

Fig. 7 Wake structure behind a moving cylinder for $f_S/f_{K0}=1$ and $X_0=0.05$; shots 1/30s apart

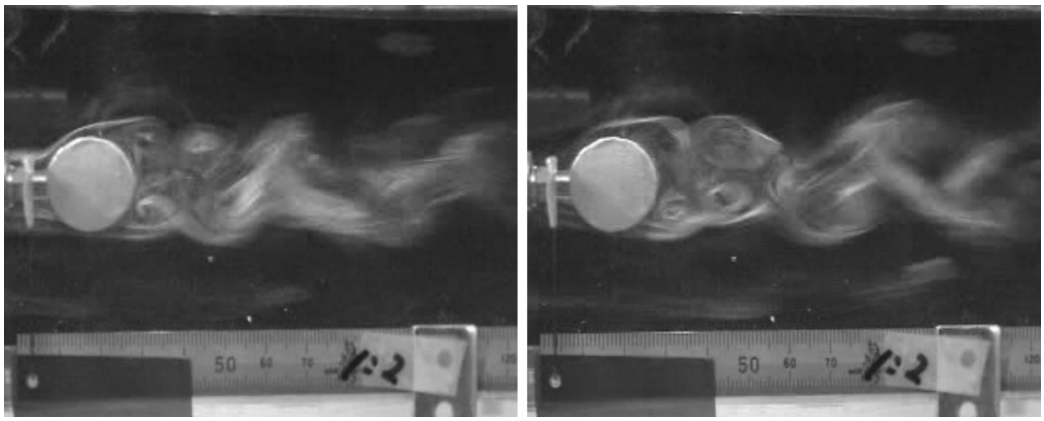

Fig. 8 Wake structure behind a moving cylinder for $f_S/f_{K0}=2$ and $X_0=0.05$

approximately reflection symmetric. This symmetry is, however, broken further downstream and accompanied by vortex merging. The result of vortex merging is an alternating wake, which

oscillates at close to the natural shedding frequency. We remark, however, that although this far wake has the same frequency as that of the wake behind a stationary cylinder, the form or structure of the wake is significantly different. Furthermore, the forced wake has characteristics of a traveling wave when viewed on video.

3. Flow symmetry considerations

3.1. The amplitude equations

In this section, we attempt a theoretical interpretation of the experimental results presented above. In particular, we wish to explain the mechanism by which the wake oscillations at half the normal Karman shedding frequency appear, when the cylinder is mechanically forced in the flow direction. The approach we take is based on the following observation. Flow symmetry plays an important role in the resulting wake dynamics; this is a finding commonly reported in most work on forced cylinder excitation as discussed in the introduction.

The global wake dynamics can be studied by investigating the symmetry changes that occur. This is a geometrical approach, as opposed to an analytical approach which would start with the Navier-Stokes equations. For external perturbations, the relation between the symmetry of these perturbations and the symmetry of the existing Karman wake pattern is key to the resulting wake behaviour.

In order to theoretically study the wake dynamics, the wake flow is described as a combination of two wake modes. One of the modes is the natural Karman shedding mode. The second is the externally imposed symmetrical mode due to forced cylinder motion. The problem now reduces to a mode interaction problem in the cylinder wake. The governing dynamics will be the solutions of the mode interaction amplitude equations. The amplitude equations may be derived in one of two ways. The aditional approach is to directly introduce the selected flow modes into the Navier-Stokes equations which then reduce to a 2-mode amplitude interaction set of equations. An alternative approach is to bypass the Navier-Stokes equations; instead, the amplitude equations can be derived (in polynomial form) based purely on the known symmetries of the interacting modes. It is this latter approach which is adopted in this work. The symmetry based approach has an important advantage. Since it is based on series expansions, low order models, which are easier to understand, can be derived. Higher order models can be derived later as the problem is better understood.

The symmetry approach, although not well known in engineering, is often implicitly used. Consider the basic problem of the buckling of a beam due to an axial load. The buckling instability is an example of a symmetry breaking instability. The straight beam has initial reflection symmetry (called $Z_2(\kappa)$, symmetry). According to equivariant bifurcation theory (the theory of bifurcations in the presence of symmetry), the $Z_2(\kappa)$-symmetry breaking problem can be reduced to the solution of a single cubic equation. The solution of this equation gives the new beam equilibrium position after buckling. This is exactly the result obtained by starting with the beam equation, introducing a compressive load and calculating the buckling load.

We start by defining the wake symmetry properties which are important for the present study. The near wake flow is idealized as follows. Prior to the initial Hopf bifurcation (which leads to the onset of Karman vortex shedding near $\mathrm{Re}_c \approx 48$), the flow has reflection symmetry, about the x-axis (directed in the flow direction). At some distance downstream of the cylinder the wake is also x-translation invariant, Fig. 9. Let the local flow velocities in the x- and y-directions be $u(x, y, t)$ and

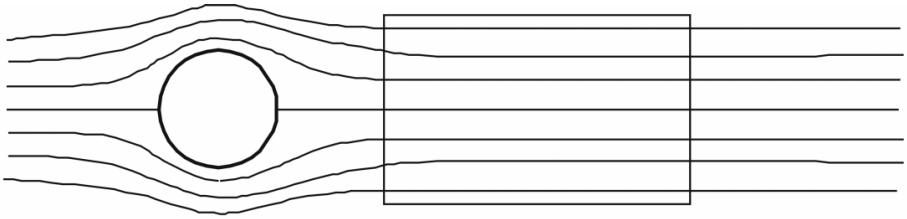

Fig. 9 Idealized wake flow with symmetry $\Gamma=Z_2(\kappa)\times SO(2)=O(2)$ in the rectangle

$v(x, y, t)$ respectively. The 2D flow symmetries above mean the following relations hold:

$$\begin{aligned} u(x, y, t) &= u(x+l, y, t) \\ u(x, y, t) &= u(x, -y, t) \\ v(x, y, t) &= 0 \end{aligned} \tag{1}$$

In symmetry theory terms, the reflection symmetry is represented as $Z_2(\kappa)$, while the translation symmetry is $SO(2)$. The overall symmetry is therefore $\Gamma=Z_2(\kappa)\times SO(2)$. Γ is therefore simply the orthogonal group, $O(2)$. Fig. 10 shows the lattice of isotropy subgroups of the base symmetry Γ. Instability and transition from a flow state with symmetry Γ to a state with 'less' symmetry involves symmetry breaking; the resulting flow symmetry must be a subgroup down the isotropy lattice. When symmetry is broken multiple solutions of lower order symmetries appear such that the summation of all the lower order symmetries, at any level of the lattice, adds up to the original base symmetry; thus 'overall' symmetry is conserved via distribution over several solutions. From Fig. 10 then, we can immediately predict, qualitatively, the types of solutions to be expected.

The symmetry subgroups D_m and $Z_2(\kappa, \pi)$ in Fig. 10 are special. They are the so called maximal isotropy subgroups. Maximal isotropy subgroups have the unique property that they are the

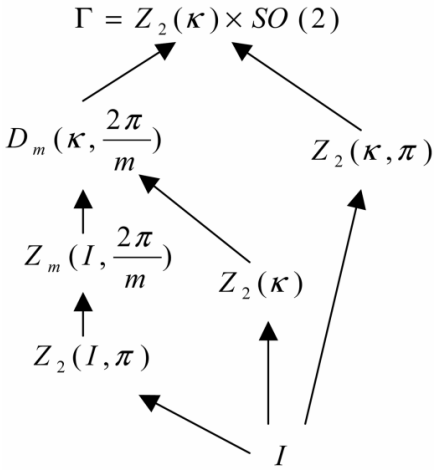

Fig. 10 Lattice of isotropy subgroups

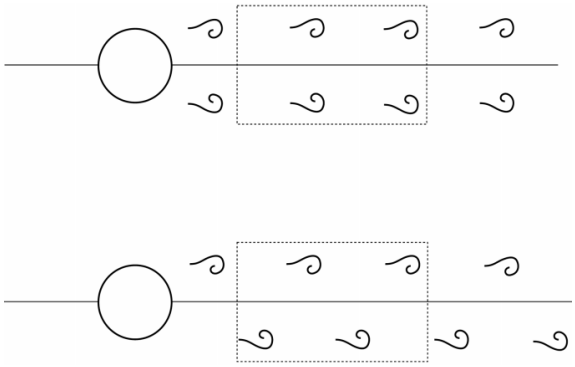

Fig. 11 The **S** and **K** wake flow modes

symmetries most likely to appear following instability from the symmetry Γ. The $Z_2(\kappa, \pi)$ symmetry is precisely the symmetry of the Karman wake mode. It is no surprise therefore that Karman shedding is ubiquitous for all bluff bodies in cross-flow. The subgroup D_m also does appear. Indeed the symmetries $Z_2(\kappa, \pi)$ and D_m (with $m=2$) are the symmetries of the well known sinuous and cosinuous 'unstable' modes found in the wake of a bluff body.

The equilibrium state (steady flow), Fig. 9, undergoes a Hopf bifurcation leading to mode **S** and/or **K**, having symmetry Γ_S and Γ_K, respectively. These modes are depicted in Fig. 11. The mode **S** velocity field satisfies the relations

$$\begin{aligned} u(x, y, t) &= u(x, -y, t) = u(x+\lambda_S, y, t) = u(x, y, t+\tau_S) \\ v(x, y, t) &= -v(x, -y, t) = -v(x+\lambda_S, y, t) = -v(x, y, t+\tau_S) \end{aligned} \tag{2}$$

For the anti-symmetric **K** mode, on the other hand

$$\begin{aligned} u(x, y, t) &= u(x, -y, t+\tau_A/2) = u(x+\lambda_K/2, -y, t) \\ v(x, y, t) &= -v(x, -y, t+\tau_A/2) = -v(x+\lambda_K/2, -y, t) \end{aligned} \tag{3}$$

The appropriate wavelength and period are represented by λ and τ, respectively. Mode **S** therefore has purely spatial symmetry Γ_S. Mode **K** on the other hand is seen to possess a mixed spatio-temporal symmetry Γ_K. The symmetries may be compactly expressed as

$$\begin{aligned} \Gamma_S &= D_m\left(\kappa, \frac{2\pi}{m}\right) \times S^1 \\ \Gamma_K &= Z_2(\kappa, \pi) \times S^1 \end{aligned} \tag{4}$$

where 'm' is the wavelength ratio λ_K/λ_S. The symmetries Γ_S and Γ_K must be subgroups of the base symmetry $\Gamma \times S^1$. Note that the circular S^1 symmetry appears as a consequence of of the periodicity associated with the Hopf bifurcation.

In the work reported here, we consider the effect of external perturbations to the Karman shedding mode. To model the resulting dynamics, Karman shedding is represented by the mode **K**. On the other hand, the external perturbations are represented by the reflection-symmetric **S** mode. Our primary goal then is to study the resulting interaction between modes **S** and **K**. As a first approximation we describe the interaction in terms of the respective modal amplitudes. Assuming that all other modes are stable, the *x*-direction velocity perturbations, for instance, may be expressed as

$$U(x, y, t)=S(t)\psi_S(y)e^{i(\lambda_S x+\omega_s t)}+K(t)\psi_K(y)e^{i(\lambda_K x+\omega_K t)}+\textit{complex conjugate} \tag{5}$$

where $S(t)$ and $K(t)$ are the mode amplitudes for mode **S** and **K**, respectively. Suppose that modes **S** and **K** destabilize via a Hopf bifurcation. We introduce a Poincare map reduction of the resulting periodic base state. The Poincare map is a simple technique for eliminating the additional dimension associated with periodic oscillations in time (or S^1 symmetry). When both modes destabilize simultaneously $\omega_S=\omega_K=\omega$ this leads to a discrete mapping in time steps of the basic modal period (here $\tau=1/\mathrm{Im}(\omega)$). The evolution of the fluid state may then be represented by a mapping of the form

$$U_{n+1}(x, y, t_{n+1}) \;=\; \Phi[U_n(x, y, t_n)] \tag{6}$$

Eq. (6) is a very compact representation of the fact the flow state U_{n+1} at time t_{n+1} is given by some function $\Phi[.]$ of the present state U_n. Note that the subscript '*n*' refers to discrete time in cycles. The function $\Phi[.]$ clearly represents all the complexity of the Navier-Stokes equations. Armed with our knowledge of the symmetry of the flow modes interacting in our experiments, we can significantly simplify the form of the function $\Phi[.]$. The resulting simplified function governs the dynamics of the restricted case of interaction between the **S** and **K** modes. The resulting equations are called amplitude equations since they give the relationship between the two modal amplitudes S_n and K_n. Substituting the coupled mode flow field (5) into (6) yields the following mode interaction amplitude equations

$$\begin{aligned} S_{n+1}&=\Phi_S(S_n, K_n)\\ K_{n+1}&=\Phi_k(K_n, S_n) \end{aligned} \tag{7}$$

where external parameter dependence (e.g., flow velocity dependence) has been suppressed. The functional forms of the mappings Φ_S, Φ_k are determined based on (i) satisfaction of conditions set by the underlying system symmetry (ii) knowledge of the existence of the initial Hopf bifurcations. Qualitatively we may describe the connection as follows. For a system having a given symmetry it is clear that the governing equations must also incorporate the same symmetry. Reflection symmetry provides a simple example. A reflection symmetric physical phenomenon is governed by an odd function satisfying the relation $f(x)=-f(-x)$. Knowing the underlying symmetry then one can derive the basic form of the governing equations. This approach is formalized by the Hilbert-Weyl theorem (see Golubitsky, *et al.* 1988, theorem 4.2). For the problem of **S**,**K**-mode interaction the authors (Mureithi, *et al.* 2002) have derived the appropriate forms of the functions Φ_S and Φ_k in Eq. (7). The resulting functions are given in the following proposition.

Proposition: Every $\Gamma = Z_2(\kappa) \times SO(2)$ - equivariant map $\Phi : C^2 \to C^2$ has the form

$$\Phi(S, K) = \begin{bmatrix} \Phi_S \\ \Phi_K \end{bmatrix} = \begin{bmatrix} p(r_1, r_2, r_3)S + q(r_1, r_2, r_3)\bar{S}^{n-1}K^m \\ r(r_1, r_2, r_3)K + s(r_1, r_2, r_3)S^n, \bar{K}^{m-1} \end{bmatrix} \text{ for } m=2k,$$
$$\Phi(S, K) = \begin{bmatrix} \Phi_S \\ \Phi_K \end{bmatrix} = \begin{bmatrix} p(r_1, r_2, r_4)S + q(r_1, r_2, r_4)\bar{S}^{2n-1}K^{2m} \\ r(r_1, r_2, r_4)K + s(r_1, r_2, r_4)S^{2n}\bar{K}^{2m-1} \end{bmatrix} \text{ for } m=2k-1 \quad (8)$$

where p, q, r, s are real polynomial functions of the $\Gamma = Z_2(\kappa) \times SO(2)$ invariants $r_1 = |S|^2$, $r_2 = |K|^2$, $r_3 = S^n\bar{K}^m$, $\bar{r}_3$ and m/n corresponds to the wavelength ratio λ_K/λ_S of the two modes. For m-odd, r_3 above should be replaced by $r_4=(S^n\bar{K}^m)^2$.

In the present work we consider the case where the symmetrical mode, **S**, is "generated" or "controlled" via forced oscillations of a cylinder in the flow direction. We then investigate the effect on Mode **K**.

3.2. Theoretical model, Case 1: wavelength ratio $\lambda_K/\lambda_S=m=1$

For this case the Poincare mapping is

$$\begin{bmatrix} \Phi_S \\ \Phi_K \end{bmatrix} = \begin{bmatrix} pS + q\bar{S}K^2 \\ rK + sS^2\bar{K} \end{bmatrix} \quad (9)$$

The amplitude mapping for the Karman mode **K** (with symmetric mode **S** amplitude as a controlled excitation 'parameter') is

$$K_{n+1} = \Phi_K(S_n, K_n) = (1 + \gamma_0 + \gamma_1|S_n|^2 + \gamma_2|K_n|^2 + ...)K_n + (\delta_0 + ...)S_n^2\bar{K}_n \quad (10)$$

where only terms up to 3rd order are considered. This equation represents the dynamics of Karman vortex shedding, subjected to external perturbations in the flow direction. Recall that we represented x-direction velocity perturbations by $U(x, y, t)$. For a stationary cylinder we can write $U(x, y, t) = K(t)\psi_K(y)e^{i(\lambda_K x + \omega_K t)} + c.c.$, where *c.c.* stands for complex conjugate. Performing measurements at a specific point $(\hat{x}, \hat{y})$ in the flow we would find that

$$U(\hat{x}, \hat{y}, t) = \bar{K}\psi_K(\hat{y})e^{i(\lambda_K\hat{x} + \omega_K t)} + c.c. \quad (11)$$

In fact we would find that the mode amplitude was constant, hence, $K(t)=\bar{K}$. The constant mode amplitude $\bar{K}$ is the steady (periodic flow) state (or fixed point) solution of Eq. (10) when $S_n=0$ thus satisfies the equation

$$\bar{K} = (1 + \gamma_0 + \gamma_2|\bar{K}|^2)\bar{K} \quad (12)$$

Note that steady state solutions of the mapping (10) therefore correspond to periodic solutions for the physical flow. Eq. (12) is the 'famous' amplitude equation derived by Landau to describe the nonlinear Karman wake oscillator. The constant γ_0 is related to the critical Reynolds number ($\mathrm{Re}_c \approx 48$) for the onset of Karman shedding. The amplitude growth rate is determined by the Landau constant γ_2. Since the onset of mode **K** is via a supercritical Hopf bifurcation we know that $\gamma_0 > 0$, $\gamma_2 < 0$.

We turn now to an analysis of the forced excitation case, $S_n \neq 0$. Introducing the parameters

$$\sigma = (\gamma_0 + \gamma_1 |S|^2), \ \mu = \delta_0 S^2, \ \gamma = \gamma_2 \tag{13}$$

Eq. (10) in polar form becomes

$$\begin{aligned} r_{n+1} &= (1 + \sigma + \mu \cos 2\phi_n) r_n + \gamma r_n^3 = f(r_n, \phi_n) \\ \phi_{n+1} &= \phi_n - \mu r_n \sin 2\phi_n \end{aligned} \tag{14}$$

with $K = re^{i\phi}$. By separating the amplitude and phase equations, a stability analysis can be easily performed. First though we note that besides the zero fixed point, Eq. (14) has fixed points given by

$$\bar{r}^2 = \left(\frac{-\sigma \pm \mu}{\gamma} \right) \tag{15}$$

Note that $K = \bar{r} e^{i\bar{\phi}}$ is an infinite set of solutions parameterized by the phase $\bar{\phi} \in \{\phi = k\pi, \ k = 1, 2, ...\}$ relative to the **S** mode. The stability of the fixed points (which correspond to periodic flow states) is dependent on the first derivative

$$\begin{aligned} f_{,r}(\bar{r}) &= 1 - 2(\sigma \pm \mu) \\ &= 1 - 2(|\gamma_0| + (\gamma_1 \pm \delta_0)|S|^2) \end{aligned} \tag{16}$$

since we have a 1-dimensional amplitude equation; an advantage of separating the phase from the amplitude equation via the polar transformation. Instability occurs when this derivative exits the unit circle, i.e., $|f_{,r}(\bar{r})| > 1$. There are 3 possible instability scenarios. For $|f_{,r}(\bar{r})| \to +1$, a pitchfork bifurcation occurs. For $|f_{,r}(\bar{r})| \to -1$, a period-doubling (or frequency halving) instability occurs. Finally, a Hopf bifurcation occurs if $f_{,r}(\bar{r})$ is a complex number and $|f_{,r}(\bar{r})| \to 1$; this latter instability introduces a second frequency in the flow.

Experimental tests by Mureithi, *et al*. (2002) have shown that $\gamma_1 \pm \delta_0 > 0$ in the physical wake flow. Based on the parameters of Eq. (10), we see that for $\gamma_1 \pm \delta_0 > 0$ we have stable periodic flow states for large enough *S*. However, increasing *S* past some critical value the fixed points undergo a period-doubling instability at $f_{,r}(\bar{r}) = -1$. Physically this means that the Karman mode **K** undergoes a period-doubling bifurcation for large enough symmetrical forcing. Physically, the instability is manifested by the appearance of flow oscillations at half the cylinder forcing frequency in the wake as observed in the experiments. Furthermore, the necessarily non-zero value of *S* breaks the Karman mode symmetry, $Z_2(\kappa, \pi)$. This is clearly visible in Fig. 7. The frames, taken half a cycle apart are not related by reflection symmetry.

3.3. Theoretical model, Case 2: wavelength ratios $1<\lambda_K/\lambda_S\leq 2$

In this section we show that the period-doubling instability is persistent in the range $1 < \lambda_K/\lambda_S \leq 2$. Consider first the intermediate wavelength ratio $\lambda_K/\lambda_S = 3/2$. This corresponds to forced cylinder oscillations at 1.5 times the vortex shedding frequency. The corresponding amplitude equation for the Karman mode is

$$K_{n+1} = \Phi_K(S_n, K_n) = (1 + \gamma_0 + \gamma_1|S_n|^2 + \gamma_2|K_n|^2 + ...)K_n + (\delta_0 + ...)S_n^4\overline{K}_n^7 \tag{17}$$

The last term on the *rhs* is of order (O(11)), clearly negligible. The equivalent polar form is similar to Eq. (14) but with the factor $\mu=0$. Thus we have

$$\begin{aligned} r_{n+1} &= (1 + \sigma)r_n + \gamma r_n^3 = f(r_n, \phi_n) \\ \phi_{n+1} &= \phi_n \end{aligned} \tag{18}$$

Eq. (18) is in fact valid for all rational ratios $1<\lambda_K/\lambda_S<2$, since in this range $\mu=0$ for a third order approximation of the amplitude equation. For $\lambda_K/\lambda_S=2$ we have a second order term $\mu=\delta_0 S$. The stability analysis of the Karman mode performed above hence remains essentially the same. It is found that, just as in Case 1, the non-zero fixed points of map (10), or the intermediate map (17,18) undergo a period-doubling bifurcation for $1<\lambda_K/\lambda_S\leq 2$. We conclude therefore, that the primary effect of mode **S** is to cause a period-doubling bifurcation of mode **K** for a wide range of excitation frequencies.

This conclusion is precisely the result found in the experiments. Period doubling was found for all wavelength ratios $1 < \lambda_K/\lambda_S\leq 2$. For wavelength ratios $\lambda_K/\lambda_S \approx 1$, the cylinder wake has a distorted wake which oscillates at half the forcing frequency. For $\lambda_K/\lambda_S = 2$ period doubling is manifested as vortex merging. The merging phenomenon is clearly visible in Fig. 8. The merged vortex street however differs from a standard Karman wake and appears to have a superposed traveling wave.

4. Conclusions

Dynamics in the wake of a solitary cylinder mechanically forced in the flow direction have been investigated both experimentally and theoretically. Experimental tests showed that inflow cylinder oscillations destabilize the alternating Karman wake leading to oscillations at half the excitation frequency.

A group theoretic analysis confirmed that interactions between modes with the present symmetries does indeed lead to a period doubling bifurcation, which is responsible for the aforementioned Karman wake instability. A remarkable result is the robustness of the period-doubling instability. It is found to occur for all wavelength ratios $1 < \lambda_K/\lambda_S \leq 2$. This result may have important consequences for the problem of Karman wake control. Perturbations in the flow direction are shown to destabilize the Karman wake. This could be used to eliminate the lock-in effect by changing the wake frequency to a value lower than the structural frequency. We note here that the symmetrical flow perturbations are not physically large. In the experiments here, the perturbations are produced with a cylinder displacement less than 0.05D. In an actual control situation, flow perturbations could be introduced via direct pressure pulsations as done in the tests by Williams *et al*. (1992). This approach is currently under investigation.

Acknowledgements

Experimental tests were conducted by T. Kashikura and S. Goda, at Kobe University, Japan. Their assistance is gratefully acknowledged.

References

Baek, S.-J., Lee, S.B. and Sung H.J. (2001), "Response of a circular cylinder wake to superharmonic excitation", *J. Fluid Mech.*, **442**, 67-88.

Baek, S.-J. and Sung, H.J. (2000), "Quasi-periodicity in the wake of rotationally oscillating cylinder", *J. Fluid Mech.*, **408**, 275.

Baek, S.-J. and Sung, H.J. (1998), "Numerical simulation of the flow behind a rotary oscillating circular cylinder", *Physics of Fluids*, **10**, 869.

Bishop, R.E.D. and Hassan, A.Y. (1963), "The lift and drag forces on a circular cylinder in a flowing fluid", *Proc. of Royal Society* (London), **A 277**, 32-50.

Golubitsky, M., Stewart, I. and Schaeffer, D.G. (1988), *Singularities and Groups in Bifurcation Theory*, Vol.II (Springer, New York).

Griffin, O.M. and Hall, M.S. (1991), "Review - vortex shedding lock-on and flow control in bluff body wakes", Trans. ASME I: *J. Fluids Eng.*, **113**, 536.

Hartlen, R.T. and Currie, I.G. (1970), "Lift-oscillator model of vortex vibration", *ASCE Proc., J. Eng. Mech. Div.*, **96**, 577-591.

Hover, F.S., Techet, A.H. and Triantafyllou, M.S. (1998), "Forces on oscillating uniform and tapered cylinders in crossflow", *J. Fluid Mech.*, **363**, 97.

King, R. (1977), "A review of vortex shedding research and its applications", *Ocean Engineering*, **4**, 141-171.

Landl, R. (1975), "A Mathematical model for vortex-excited vibrations of bluff bodies", *J. Sound Vib.*, **42**(2), 219-234.

Mureithi, N.W., Kanki, H., Goda, S., Nakamura, T. and Kashikura, T. (2002), "Symmetry breaking and mode interaction in vortex-structure interaction", Paper IMECE 2002-32512, *Proceedings, 5th International Symposium on FSI, AE & FIV+N, ASME Int'l Mech. Engrg. Congress & Exhibition*, New Orleans, Louisiana, USA.

Mureithi, N.W., Goda, S., Kanki, H. and Nakamura, T. (2001), "A nonlinear dynamics analysis of vortex-structure interaction models", *J. Pressure Vessel Technology*, **123**, 475-479.

Mureithi, N.W., Kanki, H. and Nakamura, T. 2000, "Bifurcation and perturbation analysis of some vortex shedding models", *In Flow Induced Vibrations*, eds. Ziada, S. and Staubli, T., 61-68.

Matsumoto, M. (2002), Cable aerodynamics of cable stayed bridges, in Proc. Second Int'l. Symp. On *Advances in Wind & Structures*, ed. C-K. Choi, *et al*., pp.21-42.

Mureithi, N.W. (2002), "Secondary wake mode instabilities induced by vortex-structure interaction", *In Proc. 2nd Int'l Symp. on Advances in Winds and Structures Conf.*, AWAS, Pusan, Korea.

Naudascher, E. (1987), "Flow-induced stream-wise vibrations of structures", *J. Fluids Struct.*, **1,** 265-298.

Ongoren, A. and Rockwell, D. (1988), "Flow structure from an oscillating cylinder", Part I&II., *J. Fluid Mech.*, **191,** 197-223, 225-245.

Park, D.S., Ladd, D.M. and Hendricks, E.W. (1994), "Feedback control of von Karman vortex shedding behind a circular cylinder at low Reynolds numbers", *Physics of Fluids*, **6**, 2390.

Sarpkaya, T. (1979), "Vortex-induced oscillations - A selective review", *Trans. ASME J. Appl. Mech.*, **46**, 241-258.

Shiraishi, N. (2002), "Role of aerodynamic investigation for structural design of bridges", *in Proc. Second Int'l. Symp. On Advances in Wind & Structures*, ed. C-K. Choi, *et al.* pp.3-20.

Stansby, P.K. (1976), "The locking-on of vortex shedding due to the cross-stream vibration of circular cylinders in uniform and shear flows", *J. Fluid Mech.*, **74**, 641.

Tokumaru, P.T. and Dimotakis, P.E. (1991), "Rotary oscillation control of a cylinder wake", *J. Fluid Mech.*, **224**, 77.

Williamson, C.H.K. (1987), "Three-dimensional transition in the near wake of a cylinder", *Bull. Am. Phys. Soc*., **32**, 2098.
Williamson, C.H.K. (1988), "The existence of two stages in the transition to three-dimensionality of a cylinder wake", *Physics of Fluids*, **31**, 3165.
Williamson C.H.K. (1989), "Oblique and parallel modes of vortex shedding in the wake of circular cylinder at low Reynolds number", *J. Fluid Mech.*, **206**, 579.
Williamson, C.H.K. (1996), "Vortex dynamics in a cylinder wake", *Annual Review of Fluid Mechanics*, **28**, 477.
Williamson, C.H.K. and Roshko, A. (1988), "Vortex formation in the wake of an oscillating cylinder", *J. Fluids Struct.*, **2,** 355-381.
Williams D.R., Mansy, H. and Amato, C. (1992), "The response and symmetry properties of a cylinder wake subjected to localized surface excitation", *J. Fluid Mech.*, **234,** 71-96.

CC